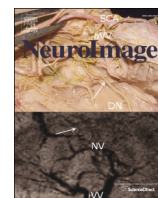




Contents lists available at ScienceDirect

NeuroImage

journal homepage: [www.elsevier.com/locate/ynimg](http://www.elsevier.com/locate/ynimg)

## Q1 Spatial attention enhances object coding in local and distributed representations of the lateral occipital complex

Q2 Matthias Guggenmos<sup>a,b,\*</sup>, Volker Thoma<sup>c</sup>, John-Dylan Haynes<sup>a</sup>, Alan Richardson-Klavehn<sup>d</sup>, Radoslaw Martin Cichy<sup>e,1</sup>, Philipp Sterzer<sup>a,b,1</sup>

<sup>a</sup> Bernstein Center for Computational Neuroscience, Berlin, Germany

<sup>b</sup> Visual Perception Laboratory, Charité Universitätsmedizin, Berlin, Germany

<sup>c</sup> School of Psychology, University of East London, London, UK

<sup>d</sup> Department of Neurology, Otto von Guericke University, Magdeburg, Germany

<sup>e</sup> Computer Science and Artificial Intelligence Laboratory, Massachusetts Institute of Technology, Cambridge, USA

### 1 0 A R T I C L E I N F O

#### Article history:

Received 30 December 2014

Accepted 1 April 2015

Available online xxxx

#### Keywords:

Attention

Objects

Lateral occipital complex

Multivariate pattern analysis

Mutual information

fMRI

### A B S T R A C T

The modulation of neural activity in visual cortex is thought to be a key mechanism of visual attention. The investigation of attentional modulation in high-level visual areas, however, is hampered by the lack of clear tuning or contrast response functions. In the present functional magnetic resonance imaging study we therefore systematically assessed how small voxel-wise biases in object preference across hundreds of voxels in the lateral occipital complex were affected when attention was directed to objects. We found that the strength of attentional modulation depended on a voxel's object preference in the absence of attention, a pattern indicative of an amplificatory mechanism. Our results show that such attentional modulation effectively increased the mutual information between voxel responses and object identity. Further, these local modulatory effects led to improved information-based object readout at the level of multi-voxel activation patterns and to an increased reproducibility of these patterns across repeated presentations. We conclude that attentional modulation enhances object coding in local and distributed object representations of the lateral occipital complex.

© 2015 Published by Elsevier Inc.

### 1. Introduction

Attention is a cognitive process that enables us to focus on certain aspects of the environment for the benefit of improved performance (Bashinski and Bacharach, 1980; Cameron et al., 2002; Carrasco et al., 2000; Hawkins et al., 1990). One way in which attention has been found to impact neural processing is through an amplification of neural responses to attended spatial locations, objects, or features (for review, see Treue, 2003). In the visual domain, attentional amplification has been found throughout the visual processing hierarchy, from the earliest stage of visual neural processing in the lateral geniculate nucleus (O'Connor et al., 2002), primary visual cortex (Gandhi et al., 1999; Martínez et al., 1999; Somers et al., 1999), up to high-level visual cortices (Murray and Wojciulik, 2004; O'Craven et al., 1999; Serences et al., 2004) and the frontal lobes (Gitelman et al., 1999). However, the nature of attentional modulation remains a topic of debate. A number of studies have reported that attention leads to a multiplicative scaling of neuronal responses (Di Russo et al., 2001; McAdams and Maunsell, 1999; Treue

and Martínez Trujillo, 1999; Treue and Maunsell, 1999), which results in an increase of a neuron's signal to noise ratio. In contrast, other studies reported results that violated the predictions of the multiplication hypothesis, by showing that spatial attention leads to increased neural responses in visual areas in the absence of any visual stimulation (Kastner et al., 1999; Luck et al., 1997; Ress et al., 2000; Silver et al., 2007). According to these studies, attentional modulation involves an unspecific baseline shift of activity.

A common approach to investigate the effects of visual attention is the recording of neural responses across a range of a stimulus parameter (e.g., orientation of motion direction) both in the presence and absence of attention. In this way, previous studies have examined the attentional modulation of single-neuron (McAdams and Maunsell, 1999; Motter, 1993; Treue and Martínez Trujillo, 1999) or voxel (Saproo and Serences, 2010, 2014) tuning profiles. However, a complicating factor for the investigation of attentional modulation in high-level object-coding areas like the human lateral occipital complex (LOC) is the lack of analogous neuronal tuning functions. Similarly, the analysis of contrast response functions – a technique that has been used to study the nature of attentional modulation for low-level visual stimuli (Reynolds et al., 2000; Williford and Maunsell, 2006) – is problematic, because object-related neuronal responses become increasingly invariant to contrast along the visual hierarchy (Avidan et al., 2002; Rolls and

\* Corresponding author at: Bernstein Center for Computational Neuroscience, Philippstraße 13, Haus 6, 10115 Berlin, Germany.

E-mail address: [matthias.guggenmos@bccn-berlin.de](mailto:matthias.guggenmos@bccn-berlin.de) (M. Guggenmos).

<sup>1</sup> Contributed equally.

Baylis, 1986) and this invariance may itself depend on attention (Murray and He, 2006). In the present work we therefore used a different approach by exploiting the fact that the LOC represents objects in a distributed fashion across ensembles of neural populations (Haxby et al., 2001; Rice et al., 2014). At the spatial resolution of fMRI this distributed code is expressed in a differential preference of voxels for a given stimulus, likely representing the cumulative stimulus preference of neurons within these voxels. Thus, if attention causes an amplification of neural activity as opposed to a mere baseline shift, these preferences should be augmented with attention, and as a consequence single- and multi-voxel responses should become more informative about the stimuli encoded in these voxels.

In the present study we presented human participants with objects under conditions of spatial attention and inattention in a functional magnetic resonance imaging (fMRI) experiment. We had two aims. First, we sought to probe the nature of attentional modulation of visual object responses in the LOC as described above, by examining whether attentional modulation increased with a voxel's preference for a given object in the absence of attention, or whether the modulation was independent of object preference. In a second step we investigated whether these local modulatory effects of attention resulted in a more informative and reliable object code. To this end we used a mutual information metric (Sapruo and Serences, 2010; Serences et al., 2009) to assess whether single-voxel responses became more informative about object identity with attention. At the multi-voxel pattern level we examined how these local changes affected the quality of object representations through pattern similarity and classification-based analyses.

## 2. Materials and methods

### 2.1. Disclosure

A previous article (Guggenmos et al., 2015) was based on the same fMRI dataset, but pursued a different research question and orthogonal analyses.

### 2.2. Participants

Eighteen healthy participants (11 female, mean age  $\pm$  SEM,  $23.4 \pm 0.8$  years) took part in the experiment for payment after giving written informed consent. The study was conducted according to the declaration of Helsinki, and approved by the local ethics committee.

### 2.3. Experimental design

Our key experimental manipulation was to direct participants' spatial attention to either an object (attended condition) or a noise stimulus (unattended condition). Overall the experimental design comprised the factors attention (attended, unattended) as a factor of interest, as well as object (camera, watering can, chair), configuration (intact, split) and side of presentation (left, right) as factors of no interest. Configuration was manipulated by minimally scrambling (half-splitting) the objects, but note that the analyses in this article were based on intact objects only. Within each of 8 experimental runs, an object appeared in 4 trials in each attention condition (in 2 trials per side of presentation). The order of presentation was randomized across the 48 trials of each run.

### 2.4. Experimental procedures

In each trial (Fig. 1A), participants viewed a stimulus display that contained an object and a noise stimulus on either side of a central fixation cross. Spatial attention was manipulated by means of a brightness discrimination task that was performed either on the object (attended condition) or the contralateral noise stimulus (unattended condition). A trial (Fig. 1A) started with a blank fixation screen for  $3300 \text{ ms} \pm 2000 \text{ ms}$ , after which one half of a central black fixation diamond turned red, indicating the side to which attention should be directed. Following this cue and a short fixed interval (250 ms), four repetitions of the stimulus–response phase appeared. Each stimulus–response phase lasted 1500 ms and comprised the presentation of the stimulus screen (500 ms), a pattern mask (133 ms) and a response screen (867 ms). The object appeared on one side of the fixation cross (offset  $3.84^\circ$  of visual angle) and a noise stimulus at the same offset on the other side of the stimulus screen. All visual stimuli subtended  $3.81$  by  $3.81^\circ$  of visual angle. A brightness change occurred 283 ms after stimulus onset simultaneously on both the object and the noise stimulus, such that they became independently and randomly either darker or lighter. Participants were instructed to press a button on the response box when the stimulus on the cued side became darker. Responses were counted as valid within a time window of 1000 ms after stimulus offset. In each repetition of the stimulus–response phase, the same object was shown at the same position. The noise stimulus, while also presented at the same position, was randomly generated for each repetition.

To independently identify object-responsive regions of the lateral occipital complex (LOC) in each participant (Malach et al., 1995), we

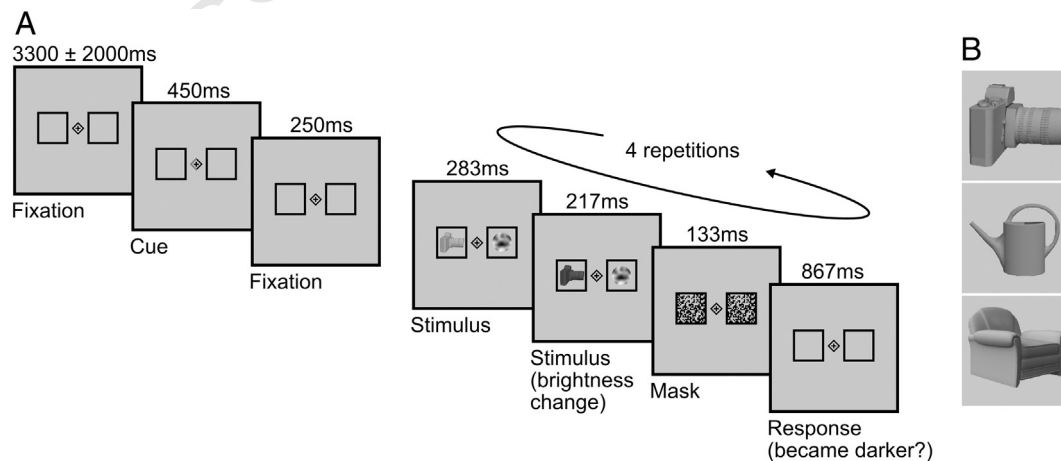


**Fig. 1.** Experimental procedures and stimuli. A. In each trial a cue indicated the side to which attention should be directed. Subsequently, four repetitions of the stimulus–response phase appeared, during each of which participants had to detect a decrease in brightness of either the object (attended condition) or the noise stimulus (unattended condition). B. The stimulus set consisted of three objects in an intact and half-split configuration.

conducted a localizer run with 5 blocks of intact objects, 5 blocks of split objects and 10 blocks of grid-scrambled versions of the objects in randomized order. Blocks lasted for 15.8 s during which 20 images were presented for 600 ms each, followed by 200 ms blank screen. Pairs of identical objects were shown left and right of fixation, equaling the configuration of the main experiment in eccentricity and size. Participants performed a one-back task on the object pairs, in which they had to indicate via button press whenever the same stimulus display appeared twice in a row.

## 2.5. Stimuli

Stimuli were generated with Psychophysics Toolbox 3 (<http://psychtoolbox.org>) and projected with a Sanyo LCD projector at 60 Hz. The stimulus set consisted of three grayscale objects (camera, watering can, chair) based on realistic three-dimensional models presented either intact or half-split (Fig. 1B). The objects were selected for representing non-overlapping man-made categories to increase the discriminability of evoked neuronal activation patterns. The noise stimuli matched the objects in terms of spatial extent and complexity to ensure that there would be no performance difference. They were randomly generated for each trial by sampling a  $9 \times 9$  random binary matrix, scaling the matrix to  $216 \times 216$  pixels, applying a low-pass filter with a cut-off frequency of 0.02/pixel and cropping pixels outside a circle of 216 pixels diameter. This procedure resulted in circular grayscale stimuli with randomly distributed smooth patches that approximately matched the objects in terms of spatial extent. Both the objects and the noise stimuli were scaled to grayscale RGB values between 50 and 205. To generate these brightness changes, the underlying RGB histograms were shifted up or down by 50 (the image background remained constant with an RGB value of 200). The pattern masks were generated for each trial by sampling an  $18 \times 18$  random binary matrix and scaling the matrix to  $216 \times 216$  pixels.

## 2.6. Eyetracking

Eyetracking data were successfully collected in 16 of 18 subjects using an infrared video eyetracking system (iView XTM MRI 50Hz, SensoMotoric Instruments, Teltow, Germany). For each run, the horizontal eye movement data were low-pass filtered and drift corrections were performed. As a measure of fixation reliability, we computed the percentage of recorded eye gaze positions during stimulus presentation within a  $1.93^\circ$  visual angle circle around the center of the fixation cross. This radius corresponded to the eccentricity of the inner edges of the two stimulus-containing boxes (see Fig. 1A). In addition, we computed the number of saccades to the intact objects and the noise stimuli, separately for the attended and the unattended condition. Saccades were defined as events of at least three consecutive data points in velocity space exceeding a velocity criterion of  $30^\circ/\text{s}$ . Saccades were counted as object-directed or noise-directed saccades, when their endpoint was located within the object-containing box, or the noise-containing box, respectively.

## 2.7. fMRI data acquisition and preprocessing

fMRI data were acquired on a 3-Tesla Siemens Trio (Erlangen, Germany) scanner using a gradient echo planar imaging (EPI) sequence and a 12-channel head-coil. We recorded 8 experimental runs of 214 whole-brain volumes each, and one LOC localizer run of 242 volumes ( $TR = 2$  s, echo time (TE) 25 ms, flip angle  $78^\circ$ , 33 slices, 3 mm isotropic resolution, interslice gap 0.75 mm). In addition, a high-resolution T1-weighted image was acquired ( $TR = 1.9$  s, echo time (TE) 2.51 ms, flip angle  $9^\circ$ , 192 slices, resolution 1 mm isotropic). The data of the experimental runs were realigned using SPM8 (Wellcome Department of Imaging Neuroscience, Institute of Neurology, London). Data analyses for the main experiment were generally performed in native subject

space. An exception was an illustrative display of the whole-brain group-level T-maps for the main effect of attention, for which we generated spatially normalized (MNI) and smoothed (8 mm Gaussian kernel) volumes. Preprocessing of the localizer data included realignment, spatial normalization to an MNI template and smoothing (8 mm Gaussian kernel).

## 2.8. fMRI data analysis

### 2.8.1. First-level general linear models (GLMs)

For each participant we estimated a GLM including the stimulus-onset regressors, accounting for the factors attention (attended, unattended), object (camera, can, chair) and configuration (intact, split). The onsets of each experimental regressor were set to the beginning of the stimulus–response phase. In addition, six motion parameters were included as regressors-of-no-interest. All experimental regressors were modeled as stick functions and convolved with a canonical hemodynamic response function.

The GLM for the functional localizer comprised regressors for objects and scrambled objects and six motion parameters. The experimental regressors were modeled as boxcar functions with durations equal to the block lengths (15.8 s) and convolved with a canonical hemodynamic response function as implemented in SPM8.

### 2.8.2. Region of interest procedures

Our region of interest (ROI) was the LOC, a functionally defined region that responds more to images of objects than their counterparts and stretches from the lateral occipital cortex to posterior fusiform gyrus (Grill-Spector et al., 1999). We anatomically constrained the LOC by a bilateral composite mask of the inferior occipital cortex, middle occipital cortex and the posterior half of the fusiform gyrus (derived from the AAL Atlas, Tzourio-Mazoyer et al., 2002). Then the LOC ROI was defined as the intersection of the anatomical mask and the functional localizer based on the t-contrast *intact objects > scrambled objects* of the functional localizer at a significance level of  $p < 0.05$  (family-wise error (FWE) corrected at the whole-brain level). Note that this t-contrast was a group-level t-contrast, because the statistical power in the first-level localizer contrasts was not sufficient to define individual ROIs in all participants at the  $p_{\text{FWE}} < 0.05$  level. To ensure a homogenous generation of the LOC ROI for all participants we thus first defined the LOC ROI in group-level (MNI) space and subsequently reverse-normalized the generated ROI to each participant's native space.

### 2.8.3. Quantifying changes in mean BOLD activity

To estimate neural activity in the LOC ROI and its dependence on attention, we extracted the voxel-wise beta values for attended and unattended objects separately and averaged across objects and voxels. This procedure resulted in single values representing the average BOLD response to attended and unattended objects.

To visualize the spatial extent of the attentional modulation at a whole-brain level, we performed a group-level repeated-measures ANOVA with factors attention and object and computed the post-hoc contrast *attended > unattended*. This analysis was based on normalized and smoothed data. Voxels were considered statistically significant at a level of  $p < 0.05$ , FWE-corrected at the whole-brain level.

### 2.8.4. Analyzing attentional modulation as a function of object preference

We next analyzed whether the attentional modulation depended on the preference of a voxel for a given object. We reasoned that if attention leads to an amplification of neural responses, the difference between a voxel's attentional modulation for the preferred object and the modulation for the non-preferred objects should increase as a function of object preference. By contrast, if attention led to an unspecific baseline shift irrespective of a voxel's preference for the presented object, the attentional modulation should not differ between the



279 presentations of the voxel's preferred and non-preferred object. We  
280 therefore defined a preference index  $PI(i)$  for each object  $i$  and each  
281 voxel based on the data of the unattended condition:

$$PI(i) = \beta_{\text{unatt}}(i) - \langle \beta_{\text{unatt}}(\setminus i) \rangle,$$

283 where  $\beta_{\text{unatt}}(i)$  and  $\beta_{\text{unatt}}(\setminus i)$  are the voxel-wise beta values in the unat-  
284 tended condition for object  $i$  and all objects except  $i$  (denoted as "not  $i$ ":  
285  $\setminus i$ ) respectively; the symbol  $\langle \rangle$  denotes the average operation (here  
286 across objects).  $PI$  was based on the unattended condition to circumvent  
287 the potential issue that the object preference of a voxel in the attended  
288 condition might not be independent of the magnitude of the attention  
289 effect. To compute the strength of the attentional modulation for an ob-  
290 ject  $i$  relative to the other objects  $\setminus i$ , we defined a relative attentional  
modulation index  $RAI(i)$  as follows:

$$RAI(i) = \beta_{\text{att}}(i) - \beta_{\text{unatt}}(i) - (\beta_{\text{att}}(\setminus i) - \beta_{\text{unatt}}(\setminus i)),$$

292 where  $\beta_{\text{att}}(i)$  and  $\beta_{\text{att}}(\setminus i)$  are the voxel-wise beta values in the attended  
condition for object  $i$  and all objects except  $i$  respectively.

293 Finally, we quantified the  $RAI$  as a function of  $PI$ . To preclude a selec-  
294 tion bias we used a leave-one-run-out procedure, such that  $PI$  and  $RAI$   
295 were computed on independent data. The leave-one-run-out procedure  
296 was performed for each object  $i$  separately as follows. In each fold, we  
297 sorted the pooled voxels from the LOC ROI according to  $PI(i)$  based on  
298 data from all but one experimental runs. We then divided the sorted  
299 voxels into 10 equinumerous bins (deciles) according to  $PI(i)$  and com-  
300 puted the average  $RAI(i)$  for the voxels in each bin based on the data of  
301 the held-out run. Subsequently, we computed an average  $RAI$  across ob-  
302 jects for each bin, resulting in a single  $RAI$  for each bin.

### 303 2.8.5. Computing the mutual information between BOLD response and pre- 304 sented objects

305 To investigate whether attention increased object information  
306 encoded in the activity of individual voxels, we used a mutual informa-  
307 tion (MI) metric. MI estimates the extent to which the uncertainty  
308 about one variable  $Y$  (here: BOLD response to the object being present-  
309 ed) is reduced by measuring another variable  $X$  (here: the object being  
310 presented) (cf. Saproo and Serences, 2010; Serences et al., 2009). The  
311 mutual information (MI) measure is defined as the difference of the  
312 total entropy  $H(X)$  and the noise entropy  $H(X|Y)$ :

$$MI(X; Y) = H(X) - H(X|Y) \\ = - \sum_{x \in X} p(x) \log_2 p(x) - \left( - \sum_{y \in Y} p(y) \sum_{x \in X} p(x|y) \log_2 p(x|y) \right).$$

314 Thus we subtract from the total entropy  $H(X)$ , which corresponds to  
315 the overall dynamic range of responses, the noise entropy, which is a  
316 measure for the noise in the data conditional on each presented object.  
317 The remainder quantifies to what degree the variation in the BOLD sig-  
318 nal is informative about the presented object. To compute the total and  
319 noise entropies, estimated BOLD responses were transformed into a dis-  
320 crete variable ( $X$ ) by dividing the entire range of responses into a set of  
321 10 equinumerous bins (deciles). This discretization was based on the  
322 pooled range of responses from all voxels in either the attended or the  
323 unattended condition after subtracting out the respective mean activa-  
324 tion levels of the attended and the unattended condition. This subtrac-  
325 tion was done to avoid errors in the binning process due to additive  
326 shifts attributed to attention (Saproo and Serences, 2010). In the  
327 above formulation,  $p(x)$  corresponds to the frequency with which a re-  
328 sponse in a given voxel falls into bin  $x$ . The noise entropy term  $H(X|Y)$   
329 additionally required the computation of the probability  $p(y)$  of each  
330 object  $y$  – 1/3 in our case, given that the experiment consisted of three  
331 equally often appearing objects – and  $p(x|y)$ , which corresponds to the  
332 frequency with which a response in a given voxel falls into bin  $x$ ,  
333 given object  $y$  was presented. We normalized the mutual information

for each participant to a range between 0 and 1 by dividing  $MI(X; Y)$  334  
by the total entropy  $H(X)$  (Kojadinovic, 2005). A normalized MI value 335  
of 0 indicates that BOLD response  $X$  and object label  $Y$  are completely in- 336  
dependent, whereas a normalized MI value of 1 indicates that response 337  
 $X$  gives complete information about the object label  $Y$ . The MI metric 338  
was applied to the responses of attended and unattended objects 339  
separately. 340

### 2.8.6. Analyzing the effects of attention at the multi-voxel pattern level 341

342 To assess the effect of attention at the multi-voxel pattern level, we  
343 examined object-related activation patterns with and without attention  
344 by means of a pattern similarity measure and support vector machine  
345 (SVM) classification. The two methods are complementary in the  
346 sense that the similarity measure provided a transparent quantification  
347 of the reproducibility (*within-object pattern similarity*) across runs,  
348 whereas the SVM classification assessed the amount of information  
349 that can be read out from these activation patterns. 349

### 2.8.7. Support vector machine classification 350

351 Support vector machine classification (SVM) was performed using  
352 *The Decoding Toolbox* (Hebart et al., 2014) with a linear C-SVM and a  
353 fixed cost parameter ( $c = 1$ ). We quantified object information in the  
354 LOC for attended and unattended objects. We trained the classifier to  
355 discriminate between objects based on multi-voxel activation patterns  
356 in the LOC ROI in native subject space (Haynes and Rees, 2005;  
357 Kamitani and Tong, 2005). A leave-one-run-out cross-validation proce-  
358 dure was used, such that in each of 8 folds the classifier was trained on  
359 the beta maps of seven runs and tested on the left out eighth run. We  
360 performed pair-wise decoding between the three pairs of objects (cam-  
361 era–can, camera–chair, can–chair) separately for the attended and the  
362 unattended condition. Subsequently the decoding accuracies were aver-  
363 aged across folds and object pairs. 363

### 2.8.8. Pattern similarity analysis 364

365 The pattern similarity analysis was based on z-transformed correla-  
366 tions between activation patterns in the LOC ROI. The *within-object pat-  
367 tern similarity* (WPS) measured the correlation between the patterns  
368 evoked by the same object across the 8 runs (separately for attended  
369 and unattended objects). For each object this led to  $8 \cdot (8 - 1) / 2 =$   
370 28 correlation coefficients for the pairwise combinations of runs,  
371 which were z-transformed and averaged across permutations and ob-  
372 jects. This procedure yielded a single within-object pattern similarity  
373 value for both the attended and the unattended condition. As a control  
374 analysis, we also computed the *between-object pattern similarity* (BPS).  
375 BPS was assessed analogously to WPS, except that the correlation coef-  
376 ficients were computed between patterns evoked by different objects,  
377 resulting in three between-object comparisons (camera–can, camera–  
378 chair, can–chair). To avoid an overestimation of pattern similarity due  
379 to within-run autocorrelations, we excluded all within-run compari-  
380 sons (Mumford et al., 2014). 380

## 3. Results 381

### 3.1. Behavioral results and fixation control 382

383 Participants detected and reported brightness changes of the objects  
384 and the noise stimuli highly accurately (performance > 98%), indicating  
385 focused attention on the correct stimulus. On average,  $98.3 \pm 0.8\%$   
386 (mean  $\pm$  SEM) of recorded eye gaze positions during stimulus presenta-  
387 tion were within the fixation area, demonstrating that the participants  
388 maintained fixation throughout the experiment. There was no difference  
389 in the overall number of saccades between the attended and the unat-  
390 tended condition (attended:  $3.1 \pm 1.6$  saccades in the experiment; unat-  
391 tended:  $3.6 \pm 2.2$ ;  $p = 0.43$ ,  $t(15) = -0.80$ , two-tailed t-test), and  
392 neither was there a difference with respect to the number of object-  
393 directed (attended:  $2.9 \pm 1.6$ ; unattended:  $0.9 \pm 0.6$ ;  $p = 0.19$ , 393

394  $t(15) = 1.36$ ) or noise-directed saccades (attended:  $0.2 \pm 0.2$ ; unattended:  $2.8 \pm 2.0$ ;  $p = 0.22$ ,  $t(15) = -1.26$ ). The interaction of saccade direction (object-directed, noise-directed) and attention (attended, unattended) was not significant ( $p = 0.21$ ,  $F(1,15) = 1.71$ , repeated-measures ANOVA). These results, as well as the low absolute number of object- or noise-directed saccades, indicate that differences between the neural correlates of the attended and the unattended condition are unlikely to ensue from effects of eye movements.

### 402 3.2. Attention amplifies responses to objects in the lateral occipital complex

403 To examine the influence of covert attention on neural activity, we compared the overall average BOLD response for attended and unattended objects within the LOC averaged over objects and sides of presentation. Attended objects led to a significant increase of neural activation ( $p < 0.001$ ,  $t(17) = 5.00$ , Cohen's  $d = 1.17$ ; Fig. 2A).

408 In order to test whether the effect of the attention manipulation was confined to object-selective cortex, we quantified the overlap between the thresholded ( $p_{\text{FWE}} < 0.05$ ) whole-brain T-maps of the contrasts *attended > unattended* (main experiment) and *intact > scrambled* (functional localizer). We found that 94.8% of the voxels showing an effect in the attention contrast overlapped with voxels classified as object-selective (Fig. 2B). Thus our focus on the LOC was justified by the spatial extent of the attentional modulation. It should be noted, however, that the attended and the unattended conditions differed only with respect to the attended stimulus type (object vs. noise pattern), but neither systematically with respect to low-level features (likely canceling out effects of attention in earlier visual areas in the contrast *attended > unattended*) nor with respect to task (likely canceling out effects of attention in executive cortices). The spatial restriction of attentional modulation to LOC therefore reflects a deliberate property of our design, rather than the absence of attentional modulation in other brain areas.

### 424 3.3. Attention modulates neural activity as a function of object preference

425 We reasoned that if attention led to an amplification of neural activity (as opposed to a mere baseline shift), the attentional modulation should be greater for a voxel's preferred object relative to its non-preferred objects. An analysis of a voxel's attentional modulation for a given object in dependence of its preference for the object should thus be informative about the specificity of the attentional modulation. To quantify the difference between the attentional modulation for preferred and non-preferred objects, we computed a relative attentional modulation index (RAI). Further, we determined a preference index (PI) for each voxel based on the mean response to a given object relative to the response of the other objects in the unattended condition. We hypothesized that RAI should increase as a function of PI.

437 To this end, we used a leave-one-run-out procedure, in which we sorted the voxels according to their PI, divided the voxels into 10 equinumerous bins (deciles) and computed the average RAI for each

bin. We found that the RAI increased as a function of PI (linear slope [mean  $\pm$  SEM]:  $0.066 \pm 0.022$ ,  $p = 0.009$ ,  $t(17) = 3.00$ , two-tailed t-test against the null hypothesis of a slope of zero; Fig. 3). In direct comparison, the average RAI for preferred objects (PI  $> 0$  [mean  $\pm$  SEM]:  $0.18 \pm 0.06$ ) was greater than the average RAI for non-preferred objects (PI  $< 0$ :  $-0.17 \pm 0.06$ ) ( $p = 0.011$ ,  $t(17) = 2.86$ , Cohen's  $d = 0.67$ ). These results show that the modulation of neural activity through spatial attention comprises an amplificatory component and is not due to a baseline shift only.

### 449 3.4. Attention increases the mutual information between BOLD responses and object identity

451 To test whether the increase of neural activity increased a voxel's information about the presented objects, we computed the mutual information for attended and unattended objects. We found that attention increased the mutual information of a voxel's responses about the objects presented ( $p < 0.001$ ,  $t(17) = 5.72$ , Cohen's  $d = 1.35$ ). The percentage of voxels showing higher mutual information in the attended relative to the unattended condition was  $55.1 \pm 0.9\%$  (mean  $\pm$  SEM across participants), which was significantly different from the chance level of 50% ( $p < 0.001$ ,  $t(17) = 5.81$ ). Thus, attention reduced the uncertainty of BOLD responses about object identity, implying enhanced object coding at the level of single voxels.

### 462 3.5. Attention enhances object representations at the pattern level

463 A growing body of evidence suggests that the LOC codes object not by means of individual neurons or neuronal populations, but across multiple distributed neuronal populations (Haxby et al., 2001; Rice et al., 2014). Thus, if attention has an enhancing effect on sensory representations, the above finding of object-specific local modulation by attention should improve the quality of multi-voxel activation patterns.

469 In a first step we assessed the effect of attention on the reproducibility of activation patterns by computing the within-object pattern similarity (WPS) of activation patterns across repeated presentations of the same object, separately for attended and unattended object presentations. We found that attention significantly increased WPS ( $p < 0.001$ ,  $t(17) = 10.51$ , two-tailed t-test; Fig. 4A), indicating that attention improved the reproducibility of responses at the pattern level. However, in a control analysis we found that attention also led to a considerable increase of the between-object pattern similarity (BPS;  $p < 0.001$ ,  $t(17) = 9.73$ , two-tailed t-test). If the increase in reproducibility for the same object (WPS) was outweighed by a simultaneous increase of the ambiguity between different objects (BPS), nothing is gained. We therefore directly compared WPS and BPS and found that the increase in WPS was greater than the increase in BPS ( $p < 0.001$ ,  $t(17) = 4.22$ ), indicating that attention led to a functionally relevant improvement of the reproducibility of multi-voxel activation patterns.

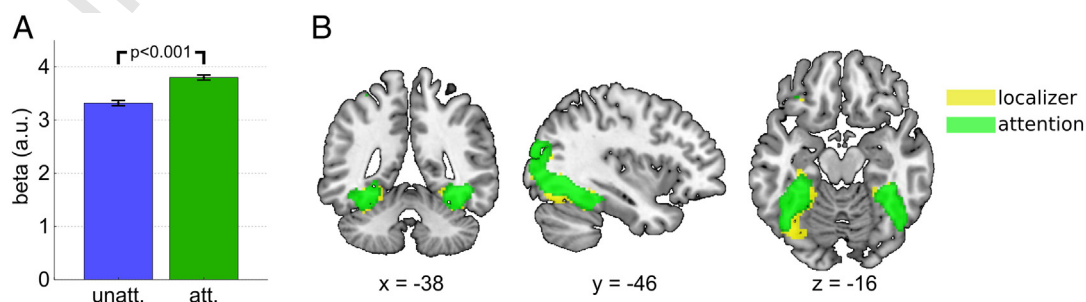


**Fig. 2.** Modulatory effect of attention. A. LOC ROI. The bars represent average beta values of the LOC ROI for the attended and unattended condition, averaged across objects and sides of presentation. Error bars denote SEM corrected for between-subject variance (Cousineau, 2005). Statistical comparison was based on a two-tailed t-test. B. Whole-brain analysis. Overlay of object-selective voxels (based on the independent functional localizer, *intact > scrambled*, thresholded at  $p_{\text{FWE}} < 0.05$ , colored in yellow) and voxels showing a significant effect of attention (*attended > unattended*, thresholded at  $p_{\text{FWE}} < 0.05$ , colored in green).

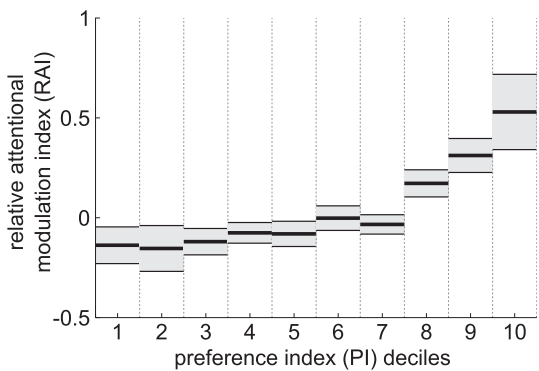


**Fig. 3.** Relative attentional modulation as a function of object preference. The relative attentional modulation index (RAI) quantifies the attentional modulation for a given object relative to the average modulation of the other objects. For each participant voxels were binned into deciles according to their object preference index (PI). The plot shows the averaged RAI for each preference bin. Error bars denote SEM corrected for between-subject variance (Cousineau, 2005).

In a second step we directly assessed how attention affected the readout of object information from the LOC by performing support vector machine classification between objects. Decoding accuracies were significantly above chance in both the attended ( $66.6\% \pm 2.0\%$ ;  $p < 0.001$ ,  $t(17) = 8.36$ , two-tailed t-test against the chance decoding accuracy of 50%) and the unattended condition ( $54.8\% \pm 1.8\%$ ;  $p = 0.017$ ,  $t(17) = 2.66$ ; Fig. 4B). Importantly, classification performance was significantly and markedly greater in the attended compared to the unattended condition ( $t(17) = 4.74$ ,  $p < 0.001$ , Cohen's  $d = 1.12$ ). Thus, the attentional modulation of neuronal responses increased object information in the LOC at the multi-voxel pattern level.

### 3.6. Enhanced readout at the pattern level is linked to the local increase in mutual information, but not mean activation

Finally, we assessed whether the attentional modulation at the single-voxel level was related to the enhancement of object representations at the pattern level. In the single-voxel-level analyses we found that attention led to an increase of (1) BOLD signal, and (2) the mutual information. We therefore correlated – across participants – both effects with the increase in decoding accuracy. We found that the increase in decoding accuracy correlated with the increase in mutual information (Pearson's  $r = 0.59$ ,  $p = 0.009$ ), but not with the increase in BOLD activation ( $r = 0.01$ ,  $p = 0.96$ ). A direct comparison confirmed that the

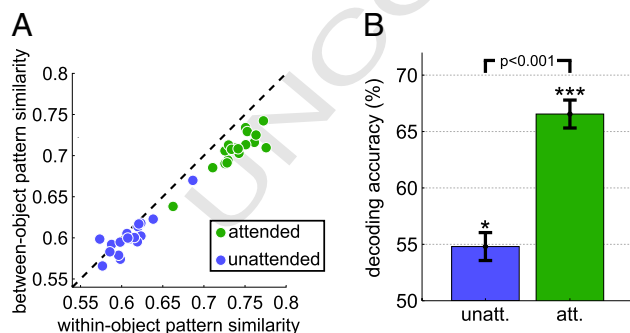


**Fig. 4.** Pattern level. A, between-object and within-object pattern similarity within the LOC ROI. Each dot represents one participant. The dashed diagonal line indicates identical within- and between-object similarity of activation patterns. Attention leads to a shift of data points below the diagonal line, indicating higher pattern similarity for repeated presentations of the same object compared to the pattern similarity of different objects. Between-subject variance was removed for illustration. B, SVM decoding results based on percent correct classification (decoding accuracy). Error bars denote SEM corrected for between-subject variance (Cousineau, 2005). Statistical comparison was based on a two-tailed t-test.

increase in mutual information explained significantly more variance than the BOLD increase ( $p = 0.034$ ,  $z\text{-score} = 2.11$ , Steiger's z-test; Steiger, 1980). Although the absence of a significant contribution of the BOLD increase is surprising (possibly caused by ceiling effects of the BOLD increase), the relationship between mutual information and decoding accuracy suggests that the local attentional modulation of neuronal responses increases the information content of object representations at the pattern level.

## 4. Discussion

We examined tuning-dependent attentional modulation of object representations in the LOC and the resulting enhancement of object representations at the single-voxel level and the multi-voxel pattern level. At the single-voxel level we found that (1) responses in the LOC were considerably stronger when an object was attended relative to when a noise stimulus was attended; (2) the relative attentional modulation (the attentional modulation for a given object relative to the average modulation of other objects) increased as a function of a voxel's preference for the given object; and (3) mutual information between a voxel's responses and object identity increased, demonstrating that responses became more informative about a presented object when the object was attended compared to when it was unattended. All three results provide evidence against a mere baseline-shift effect of attention. Further analyses showed that these local changes resulted in increased object information at the level of multi-voxel patterns and increased similarity of these patterns across multiple presentations, indicating increased reproducibility of distributed neuronal responses.

### 4.1. Effects of attention at the level of individual voxels

A key goal of this study was to investigate whether the observed increase in activity involved amplificatory attentional modulation, or merely an unspecific baseline shift. Previous neuroimaging studies reported that neural activity increased with attention in high-level visual cortex (Baldauf and Desimone, 2014; Connor et al., 1997; Murray and Wojciulik, 2004; O'Craven et al., 1999; Serences et al., 2004), and showed that the effects of attention were specific to coarse functional modules, such as parahippocampal place area (PPA) or fusiform face area (FFA). However, given that objects are known to be coded across distributed neuronal ensembles in visual cortex (Haxby et al., 2001; Rice et al., 2014), it is desirable to analyze attentional modulation at a more fine-grained level, thereby accounting for the differential tuning of neuronal populations within these areas. Here we provide evidence for voxel-wise object-specific attentional modulation of responses in the LOC by identifying a relationship between attentional modulation and object preference. The consistent increase of the relative attentional modulation across preference levels suggests that subtle difference in preference measured in the absence of attention became amplified as attention was directed to the objects. Our additional information-theoretic analyses indicated that such attentional modulation effectively increased the information of voxel-wise responses about object identity, in line with previous work on orientation coding in V1, which likewise found an increase in mutual information with attention (Saproo and Serences, 2010).

How do these results relate to the multiplicative gain hypothesis of attention derived from neurophysiological recordings in monkeys (McAdams and Maunsell, 1999; Treue and Martínez Trujillo, 1999)? It should be noted that a direct comparison between the BOLD responses in our study and spiking activity in these previous studies is difficult for two reasons: first, BOLD responses are more closely related to the local field potentials and hence synaptic activity than to spiking neuronal activity (Ekstrom, 2010; Logothetis, 2003; Logothetis et al., 2001); and second, efficient event-related fMRI designs such as ours do not permit inferences about the absolute level of stimulus-related BOLD activity, which would be necessary to quantify the ratio between attended and



569 unattended responses analogous to the ratio of firing rates in these previous  
 570 neurophysiological studies. Nevertheless, our results do provide  
 571 indirect evidence for the multiplicative gain as opposed to a mere baseline  
 572 shift hypothesis. Consider the result of increased attentional modulation  
 573 with object preference. A voxel's preference for a given object  
 574 may indicate that, for a fixed number of neurons tuned to different objects,  
 575 the tuning curves of neurons are biased more towards the given object than  
 576 to the other objects. Alternatively, it may indicate that for a fixed bias  
 577 towards the given object an overall greater number of neurons prefer the  
 578 given object. Importantly, in both cases an unspecific baseline shift would  
 579 lead to an equal increase of neural activity for preferred and non-preferred  
 580 objects, which is at odds with our results. To illustrate why the increase in  
 581 MI provides evidence for a multiplicative gain mechanism as opposed to a  
 582 pure baseline shift explanation, it is helpful to consider two objects A and B  
 583 and a hypothetical voxel consisting of neurons with a preference for, e.g.,  
 584 object A. In case of a pure baseline shift the voxel would show increased  
 585 responses to both objects and neural responses would therefore not become  
 586 more informative about whether object A or B was presented. In contrast,  
 587 in case of multiplicative scaling, attention will lead to greater response  
 588 amplification for object A compared to object B, increasing the dynamic  
 589 range of responses and resulting in increased mutual information between  
 590 neural responses and presented objects. Thus, the increase in mutual  
 591 information by attention provides a second line of evidence in favor of a  
 592 multiplicative gain mechanism and against a pure baseline shift  
 593 explanation.  
 594

#### 595 4.2. Effects of attention at the multi-voxel pattern level

596 At the level of multi-voxel activation patterns we found improved  
 597 decodability of attended relative to unattended objects, which is in  
 598 accordance with similar reports for early (Jehee et al., 2011; Kamitani  
 599 and Tong, 2005) and high-level visual areas (Pratte et al., 2013; Reddy  
 600 and Kanwisher, 2007). This result demonstrates that the attentional  
 601 modulation increased the information content of distributed object  
 602 representations in the LOC, potentially benefitting information readout  
 603 from the LOC by high-level executive cortices. An analysis of pattern  
 604 similarity showed that attention increased the reproducibility of activation  
 605 patterns of the same object. Such an increase in reproducibility would  
 606 be expected on the assumption of a multiplicative attentional scaling  
 607 mechanism, where neuronal responses become amplified without an  
 608 equivalent increase of the noise (which increases as the square-root of  
 609 the signal). Another possibility is that the increase in reproducibility is  
 610 the result of more discrete neural processing with attention, as proposed  
 611 for conscious relative to non-conscious percepts (Sackur and Dehaene,  
 612 2009; Schurger et al., 2010). When discrete decisions are reached at  
 613 each (object) processing stage, before they are dispatched to the next  
 614 stage, the resulting activation patterns might become more stereotypical  
 615 and reproducible.

616 A number of previous fMRI studies have used MVPA to study the effects  
 617 of attention on neural responses (Esterman et al., 2009; Jiang et al.,  
 618 2013; Pratte et al., 2013; Reddy and Kanwisher, 2007; Reddy et al.,  
 619 2009; Tamber-Rosenau et al., 2011). In particular, Reddy and  
 620 Kanwisher (2007) and Reddy et al. (2009) investigated the decodability  
 621 of complex stimuli in high-level visual cortex when they were presented  
 622 alongside a second object and were either attended or unattended.  
 623 Reddy and Kanwisher (2007) found that information about object categories  
 624 encoded in multi-voxel activation patterns was strongly reduced to the  
 625 point of being abolished when attention was diverted. In the present  
 626 study we showed that multi-voxel responses were reduced, but still  
 627 informative about object categories even when attention was diverted.  
 628 This difference may be explained by the fact that participants in the  
 629 study by Reddy and Kanwisher (2007) directed their attention to complex  
 630 distractor stimuli (which, in addition, were the relevant stimuli in  
 631 other trials), whereas participants in our study viewed noise stimuli in  
 632 the unattended condition. It is conceivable that the absence of high-

633 level visual cortex information for unattended objects in Reddy and  
 634 Kanwisher (2007) was caused by distractor-related neural responses  
 635 interfering with the activation pattern of the unattended target object.  
 636 Along similar lines, Reddy et al. (2009) interpreted the informational  
 637 gain for attended objects (or loss for unattended objects) in the biased  
 638 competition framework. According to this view, attention serves to  
 639 disambiguate the overlapping multi-voxel patterns of different objects  
 640 through a shift towards the pattern of the currently attended object.  
 641 Aside from investigating the effect of attention in sensory cortices,  
 642 other studies have successfully used MVPA to study the initiation and  
 643 control of attentional shifts. For instance, Esterman et al. (2009) and  
 644 Tamber-Rosenau et al. (2011) showed that spatial patterns of brain  
 645 activity within the medial superior parietal lobule reliably differentiated  
 646 between several domains of cognitive attentional control at a given  
 647 moment. Thus, in our and previous studies, MVPA presented a powerful  
 648 technique to probe distributed neural underpinnings of different  
 649 attentional phenomena, from the initiation of attentional shifts to the  
 650 modulation of sensory representations.

#### 651 4.3. Linking the single-voxel and the multi-voxel pattern level

652 Finally, we linked the effects of attention at the single-voxel level  
 653 with the effects at the pattern levels by correlating the increase in  
 654 decoding accuracy of multi-voxel activation patterns to the increase in  
 655 either BOLD signal or mutual information. Unexpectedly, we found  
 656 that the increase in mean activation was not related to the increase in  
 657 decoding accuracy. This negative finding could indicate that the  
 658 attentional manipulation in our paradigm operated in a range, in which  
 659 effects at the pattern level were insensitive to the overall magnitude  
 660 (e.g., because the BOLD increase was at maximum). Alternatively, as  
 661 the overall effect of attention likely involves both a multiplicative  
 662 component and a baseline shift, the unspecific baseline shift component  
 663 might have masked the effect of the relevant multiplicative component.  
 664 In contrast, we found that the increase in mutual information explained  
 665 a considerable amount of variance of improvements in pattern-based  
 666 decoding. This result demonstrates that the increase of object information  
 667 at the single-voxel level substantially translated to an enhanced object  
 668 code at the pattern level. This link is informative, as the information  
 669 content encoded in the linear combination of voxels can show strong  
 670 gains, while information encoded in the individual voxel may show  
 671 only small changes (for examples of such scenarios see Haynes and  
 672 Rees, 2006). It is currently not clear whether the distributed object  
 673 code in LOC represents the immediate neural correlate of perception,  
 674 or whether it reflects object processing prior to perception. In either  
 675 case our data indicate that the enhancement of sensory representations  
 676 through attention – which may directly or indirectly underlie perceptual  
 677 improvements – is not a phenomenon that solely emerges at the level  
 678 of distributed object fingerprints. Instead, the improvement in pattern  
 679 decoding likely represents the cumulative result of informational gains  
 680 in multiple local units of LOC.

#### 681 4.4. Implications for mechanisms of visual attention

682 The results of the present study corroborate the notion that behavioral  
 683 benefits of attention are based on an enhanced stimulus processing in  
 684 sensory brain areas (Bisley, 2011). Our finding that the magnitude of  
 685 attentional modulation increased with object preference suggests a  
 686 response gain mechanism that magnifies stimulus-driven responses as a  
 687 function of response strength without attention. Importantly, our  
 688 information-theoretic analyses demonstrate that the attentional modulation  
 689 effectively increases object information encoded in high-level visual  
 690 cortex, which may facilitate the readout in executive cortices and thus  
 691 benefit perceptual decision making. A unifying theoretical framework  
 692 for such attentional modulation of neural activity is provided by the  
 693 normalization model of attention (Reynolds and Heeger, 2009).  
 694 The model describes the modulation of attention by two processes: a

695 multiplication of neuronal responses by an attention field and a division  
 696 (normalization) by a suppressive drive. Thus, our observed differences  
 697 between neural responses to attended and unattended objects may  
 698 not only be caused by a boost of neural processes tuned to the attended  
 699 object, but also by a suppression of activity related to the unattended  
 700 object. Another key aspect of the model is that it makes specific predic-  
 701 tions regarding the effect of different attentional strategies on neural ac-  
 702 tivity. According to the model, a purely spatial attention strategy causes  
 703 a scaling of the entire tuning curves (because the attention field is then  
 704 assumed to be constant across feature dimensions), whereas a purely  
 705 feature-based attention strategy causes a sharpening of tuning curves.  
 706 The fact that our brightness discrimination task emphasized spatial at-  
 707 tention strategies over feature-based strategies may thus explain the  
 708 strong amplitude modulation of the BOLD response in our study. Future  
 709 neuroimaging studies could test whether our findings of tuning-  
 710 dependent attentional modulation and information-theoretic gains  
 711 through endogenous visual spatial attention generalize to other forms  
 712 of attention, e.g. to involuntary (exogenous) shifts of attention or to  
 713 other sensory modalities.

714 In conclusion, our results show that visual spatial attention modu-  
 715 lates neural activity as a function of voxel-based object preferences.  
 716 Through these modulatory processes, attention enhances object coding  
 717 both at the single-voxel and pattern level, which may give rise to im-  
 718 proved perception and perceptual decisions.

## 719 Acknowledgments

720 This research was supported by the German Research Foundation  
 721 (DFG) through the Research Training Group GRK1589/1 (to M.G. and  
 722 P.S.), and Grants STE1430/6-1 (to P.S.), and RI1847/1-1 and  
 723 SFB779TPA10N (to A.R.-K). R.C. was funded by a Feodor Lynen Grant  
 724 of the Alexander von Humboldt Foundation. We thank Guy Middleton  
 725 for assistance with rendering the object images from 3D models.

## 726 References

- 727 Avidan, G., Harel, M., Hendler, T., Ben-Bashat, D., Zohary, E., Malach, R., 2002. Contrast sensitivity  
 728 in human visual areas and its relationship to object recognition. *J. Neurophysiol.* 87,  
 729 3102–3116.  
 730 Baldauf, D., Desimone, R., 2014. Neural mechanisms of object-based attention. *Science* 344,  
 731 424–428.  
 732 Bashinski, H.S., Bacharach, V.R., 1980. Enhancement of perceptual sensitivity as the result of se-  
 733 lectively attending to spatial locations. *Percept. Psychophys.* 28, 241–248.  
 734 Bisley, J.W., 2011. The neural basis of visual attention. *J. Physiol.* 589, 49–57.  
 735 Cameron, E.L., Tai, J.C., Carrasco, M., 2002. Covert attention affects the psychometric function of  
 736 contrast sensitivity. *Vis. Res.* 42, 949–967.  
 737 Carrasco, M., Penpeci-Talgar, C., Eckstein, M., 2000. Spatial covert attention increases contrast  
 738 sensitivity across the CSF: support for signal enhancement. *Vis. Res.* 40, 1203–1215.  
 739 Connor, C.E., Preddie, D.C., Gallant, J.L., Essen, D.C. Van, 1997. Spatial attention effects in macaque  
 740 area V4. *J. Neurosci.* 17, 3201–3214.  
 741 Cousineau, D., 2005. Confidence intervals in within-subject designs: a simpler solution to Loftus  
 742 and Masson's method. *Tutor. Quant. Methods Psychol.* 1, 42–45.  
 743 Di Russo, F., Spinelli, D., Morrone, M.C., 2001. Automatic gain control contrast mechanisms are  
 744 modulated by attention in humans: evidence from visual evoked potentials. *Vis. Res.* 41,  
 745 2435–2447.  
 746 Ekstrom, A., 2010. How and when the fMRI BOLD signal relates to underlying neural activity: the  
 747 danger in dissociation. *Brain Res. Rev.* 62, 233–244.  
 748 Esterman, M., Chiu, Y., Tamber-rosenau, B.J., Yantis, S., 2009. Decoding cognitive control in  
 749 human parietal cortex. *Proc. Natl. Acad. Sci. U. S. A.* 106, 17974–17979.  
 750 Gandhi, S.P., Heeger, D.J., Boynton, G.M., 1999. Spatial attention affects brain activity in human  
 751 primary. *Proc. Natl. Acad. Sci. U. S. A.* 96, 3314–3319.  
 752 Gitelman, D.R., Nobre, A.C., Parrish, T.B., LaBar, K.S., Kim, Y.H., Meyer, J.R., Mesulam, M., 1999. A  
 753 large-scale distributed network for covert spatial attention: further anatomical delineation  
 754 based on stringent behavioural and cognitive controls. *Brain* 122, 1093–1106.  
 755 Guggenmos, M., Thoma, V., Cichy, R.M., Haynes, J.-D., Sterzer, P., Richardson-Klavehn, A., 2015.  
 756 Non-holistic coding of objects in lateral occipital complex with and without attention.  
 757 *NeuroImage* 107, 356–363.  
 758 Hawkins, H.L., Hillyard, S.A., Luck, S.J., Mouloua, M., Downing, C.J., Woodward, D.P., 1990. Visual  
 759 attention modulates signal detectability. *J. Exp. Psychol. Hum. Percept. Perform.* 16,  
 760 802–811.  
 761 Haxby, J.V., Gobbini, M.I., Furey, M.L., Ishai, A., Schouten, J.L., Pietrini, P., 2001. Distributed and  
 762 overlapping representations of faces and objects in ventral temporal cortex. *Science* 293,  
 763 2425–2430.  
 764 Haynes, J.-D., Rees, G., 2005. Predicting the orientation of invisible stimuli from activity in  
 765 human primary visual cortex. *Nat. Neurosci.* 8, 686–691.

- Haynes, J.-D., Rees, G., 2006. Decoding mental states from brain activity in humans. *Nat. Rev.* 766  
*Neurosci.* 7, 523–534.  
 Hebart, M.N., Görgen, K., Haynes, J.-D., 2014. The Decoding Toolbox (TDT): a versatile software 767  
 package for multivariate analyses of functional imaging data. *Front. Neuroinform.* 8, 769  
 Jehee, J.F.M., Brady, D.K., Tong, F., 2011. Attention improves encoding of task-relevant features in 770  
 the human visual cortex. *J. Neurosci.* 31, 8210–8219.  
 Jiang, J., Summerfield, C., Egner, T., 2013. Attention sharpens the distinction between expected 772  
 and unexpected percepts in the visual brain. *J. Neurosci.* 33, 18438–18447.  
 Kamitani, Y., Tong, F., 2005. Decoding the visual and subjective contents of the human brain. 774  
*Nat. Neurosci.* 8, 679–685.  
 Kastner, S., Pinsk, M.A., De Weerd, P., Desimone, R., Ungerleider, L.G., 1999. Increased activity in 776  
 human visual cortex during directed attention in the absence of visual stimulation. *Neuron* 777  
 22, 751–761.  
 Kojadinovic, I., 2005. On the use of mutual information in data analysis: an overview. *Proceed-* 779  
*ings of the 11th International Symposium on Applied Stochastic Models and Data Analysis* 780  
 (ASMDA '05), pp. 738–747.  
 Logothetis, N.K., 2003. The underpinnings of the BOLD functional magnetic resonance imaging 782  
 signal. *J. Neurosci.* 23, 3963–3971.  
 Logothetis, N.K., Pauls, J., Augath, M., Trinath, T., Oeltermann, A., 2001. Neurophysiological inves- 784  
 tigation of the basis of the fMRI signal. *Nature* 412, 150–157.  
 Luck, S.J., Chelazzi, L., Hillyard, S.A., Desimone, R., 1997. Neural mechanisms of spatial selective 786  
 attention in areas V1, V2, and V4 of macaque visual cortex. *J. Neurophysiol.* 77, 24–42.  
 787  
 788  
 789  
 790  
 791  
 792  
 793  
 794  
 795  
 796  
 797  
 798  
 799  
 800  
 801  
 802  
 803  
 804  
 805  
 806  
 807  
 808  
 809  
 810  
 811  
 812  
 813  
 814  
 815  
 816  
 817  
 818  
 819  
 820  
 821  
 822  
 823  
 824  
 825  
 826  
 827  
 828  
 829  
 830  
 831  
 832  
 833  
 834  
 835  
 836  
 837  
 838  
 839  
 840  
 841  
 842  
 843  
 844  
 845  
 846  
 847  
 848  
 849  
 850  
 851  
 852  
 853  
 854  
 855  
 856  
 857  
 858  
 859  
 860  
 861  
 862  
 863  
 864  
 865  
 866  
 867  
 868  
 869  
 870  
 871  
 872  
 873  
 874  
 875  
 876  
 877  
 878  
 879  
 880  
 881  
 882  
 883  
 884  
 885  
 886  
 887  
 888  
 889  
 890  
 891  
 892  
 893  
 894  
 895  
 896  
 897  
 898  
 899  
 900  
 901  
 902  
 903  
 904  
 905  
 906  
 907  
 908  
 909  
 910  
 911  
 912  
 913  
 914  
 915  
 916  
 917  
 918  
 919  
 920  
 921  
 922  
 923  
 924  
 925  
 926  
 927  
 928  
 929  
 930  
 931  
 932  
 933  
 934  
 935  
 936  
 937  
 938  
 939  
 940  
 941  
 942  
 943  
 944  
 945  
 946  
 947  
 948  
 949  
 950  
 951  
 952  
 953  
 954  
 955  
 956  
 957  
 958  
 959  
 960  
 961  
 962  
 963  
 964  
 965  
 966  
 967  
 968  
 969  
 970  
 971  
 972  
 973  
 974  
 975  
 976  
 977  
 978  
 979  
 980  
 981  
 982  
 983  
 984  
 985  
 986  
 987  
 988  
 989  
 990  
 991  
 992  
 993  
 994  
 995  
 996  
 997  
 998  
 999  
 1000